JCTC Journal of Chemical Theory and Computation

Human Cytomegalovirus Protease: Why is the Dimer Required for Catalytic Activity?

César Augusto Fernandes de Oliveira,*,†,§ Cristiano Ruch Werneck Guimarães,‡,∥ Gabriela Barreiro,‡,⊥ and Ricardo Bicca de Alencastro†

Physical Organic Chemistry Group, Departamento de Química Organica, Instituto de Química, Universidade Federal do Rio de Janeiro, Cidade Universitária, CT, Bloco A, lab. 609, Rio de Janeiro, RJ 21949-900, Brazil, and Department of Chemistry, Yale University, 225 Prospect St., New Haven, Connecticut 06520-8107

Received May 18, 2006

Abstract: Human cytomegalovirus (HCMV) is a pathogenic agent responsible for morbidity and mortality in immunocompromised and immunosuppressed individuals. HCMV encodes a serine protease that is essential for the production of infectious virions. In this work, we applied molecular dynamics (MD) simulations on HCMV protease models in order to investigate the experimentally observed (i) catalytic activity of the enzyme homodimer and (ii) induced-fit mechanism upon the binding of substrates and peptidyl inhibitors. Long and stable trajectories were obtained for models of the monomeric and dimeric states, free in solution and bound covalently and noncovalently to a peptidyl-activated carbonyl inhibitor, with very good agreement between theoretical and experimental results. The MD results suggest that HCMV protease indeed operates by an induced-fit mechanism. Also, our analysis indicates that the catalytic activity of the dimer is a result of more favorable interactions between the oxyanion in the covalently bound state and the backbone nitrogen of Arg165, resulting in a reaction that is 7.0 kcal/mol more exergonic and a more significant thermodynamic driving force. The incipient oxyanion in the transition state should also benefit from the stronger interactions with Arg165, reducing in this manner the intrinsic activation barrier for the reaction in the dimeric state.

Introduction

Herpesviruses are responsible for several health problems in humans and in most species in the animal kingdom.[1] All of the herpesviruses are members of one family, the Herpesviridae, and have certain common characteristics such as their ability to establish latency during primary infection.[2] The human herpesviruses have been classified into three subfamilies designated α, β, and γ. The α subfamily includes herpes simplex virus type 1, herpes simplex virus type 2, and the varicella-zoster virus. The β-herpesviruses include human cytomegalovirus (HCMV) and human herpesviruses 6 and 7. The γ subfamily, which is specific for either B or T lymphocytes, includes Epstein−Barr and Kaposi's sarcoma-associated herpesvirus, also known as human herpesvirus 8.[3]

HCMV is a highly species-specific DNA virus infecting up to 80% of the general population, though most of these infections are clinically asymptomatic.[4] HCMV is a leading opportunistic infectious pathogen in individuals with suppressed or compromised immune systems, causing several health problems such as pneumonia, retinitis, and death.[4,5]

* Corresponding author fax: (858) 534-4974; e-mail: cesar@mccammon.ucsd.edu.
† Universidade Federal do Rio de Janeiro.
‡ Yale University.
§ Current address: Department of Chemistry and Biochemistry, University of California, San Diego, 9500 Gilman Drive, La Jolla, CA 92093.
∥ Current address: Amgen, Inc., 1120 Veterans Boulevard, South San Francisco, CA 94080.
⊥ Current address: Department of Pharmaceutical Chemistry, University of California, San Francisco, 600 16th St., San Francisco, CA 94143.

10.1021/ct600175x CCC: $37.00
Published on Web 11/29/2006

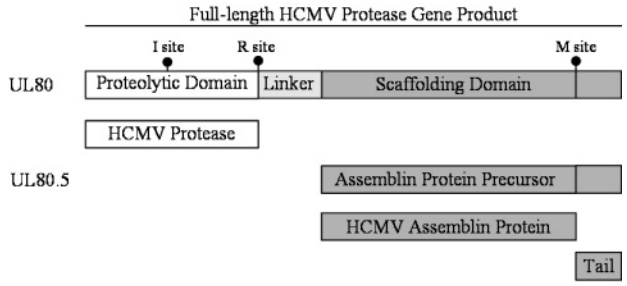

Figure 1. Maturational processing of HCMV protease and the assembly protein.

Because the number of organ transplantations and people infected with HIV has increased considerably in the past decades, the search for effective antiviral treatments is of vital importance.[5,6] HCMV is also very common in neonates, infecting 1% of newborn infants. It is estimated that 10% of these are symptomatic and may experience severe sequelae such as mental retardation and hearing disturbances.[5,7] Current treatment options for HCMV infections in clinical use include ganciclovir, valganciclovir, foscarnet, cidofovir, and formivirsen.[5] Although these HCMV DNA-polymerase inhibitors potently reduce viral replication, they exhibit toxicity and require intravenous administration to attain therapeutic levels. Moreover, viral resistance to current drugs is becoming an increasingly serious problem.[8,14]

All members of the herpesvirus family encode a protease that participates in the maturation of the viral capsid, whose activity is essential for the production of infectious virions.[15−17] Although it has only been demonstrated for herpes simplex virus type 1,[17] on the basis of homology, the protease is assumed to be essential in other herpesviruses. The extensive number of recently published articles aimed at obtaining inhibitors of the HCMV protease shows that this enzyme became an attractive target for the development of anti-herpes agents.[4,7,15,18−26]

The viral genome contains the open reading frame UL80, which encodes the full-length 80 kDa herpesvirus protease and its substrate.[15,27] Full-length HCMV protease is composed of an N-terminal 256-amino-acid proteolytic domain, a linker region, and a C-terminal structural domain, the scaffolding domain (Figure 1). In HCMV, the assemblin protein precursor (UL80.5 gene product) interacts with the major capsid protein and acts as a scaffold in the nucleus around which the capsid assembles.[28,29] To allow for the packaging of viral DNA, the full-length protease UL80 gene product undergoes autoproteolytic cleavage at the maturation site (M-site) and the release site (R-site) of the scaffolding domain. In the case of HCMV, the protease catalyzes an additional cleavage at the I-site.[30,31] The M-site, near the carboxy terminus, removes the carboxy tail from the scaffolding domain and from the assemblin protein precursor, while the R-site releases the N-terminal fragment (proteolytic domain) from the full-length protease gene product. The proteolytic domain fragment retains all the catalytic activity of the full-length protease protein and is generally referred to as HCMV protease.[32] The I-site produces a two-chain form of the protease that is still catalytically active.[30,31]

Chart 1. Peptidyl-Activated Carbonyl Inhibitor Used in This Work[a]

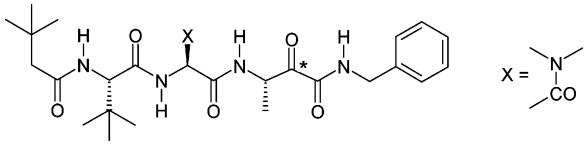

[a] The starred atom corresponds to the carbon attacked by Ser132.

Biochemical and mutagenesis studies have identified the herpesvirus protease as a serine protease, though its sequence does not bear any homology to other serine proteases or other proteins in general.[15,33] Its unusual amino acid sequence and biochemical properties establish the herpesvirus protease as a new class of serine proteases.[34−40] In HCMV, X-ray crystallographic studies revealed that the protease possesses a unique polypeptide backbone fold and catalytic triad;[38−41] the third member is a His residue (Ser132, His63, and His157), whereas classical serine proteases have either an Asp or Glu residue.[42−46] In addition, this enzyme has been shown to operate by an induced-fit mechanism, in contrast to classical serine proteases where substrate binding has generally little impact on the protein conformation.[47−50] Finally, although crystallographic data indicates that each monomeric subunit possesses a well-separated and complete active site, biochemical studies showed that dimerization is required for catalytic activity.[47,51,52]

In this work, we performed long molecular dynamics (MD) simulations on HCMV protease models to study the experimentally observed induced-fit mechanism operated by the enzyme. More specifically, we aimed at investigating if the binding of a peptidyl-activated carbonyl inhibitor (Chart 1),[47] prior to covalent adduct formation, induces conformational changes on the enzyme that would bring it to a catalytically active form. Another goal was to understand the structural and energetic factors responsible for the catalytic activity of the enzyme dimer. The current study is a more complete account of the work previously published by our group.[50]

Computational Details

The crystal structure of HCMV protease in complex with the peptidomimetic inhibitor BILC 821 (PDB code: 2WPO) was used to build our protease models.[48] The crystal structure contains residues 4−46, 53−143, 152−200, and 210−256 for each of four monomers of the protease belonging to two separate dimers with one inhibitor bound covalently to each protease monomer. Because we are currently interested in determining the structural and energetic requisites that govern the activation of the HCMV protease dimeric form and in studying the conformational changes that occur in the protein prior to and after the covalent adduct formation, six different models have been considered: the dimeric and monomeric forms free in solution (**D** and **M**, respectively) and complexed noncovalently (**DI** and **MI**) and covalently (**D-I** and **M-I**) to a peptidyl-activated carbonyl inhibitor (Chart 1), very similar to BILC 821.[48] The 26 residues of the HCMV protease not observed in the monomers of the crystal structure are in the following regions: 1−3 at the N terminus of the enzyme, which form a small helix (named αN), 47−52 at loop L3, 144−151 at loop L9, and 201−209 at loop

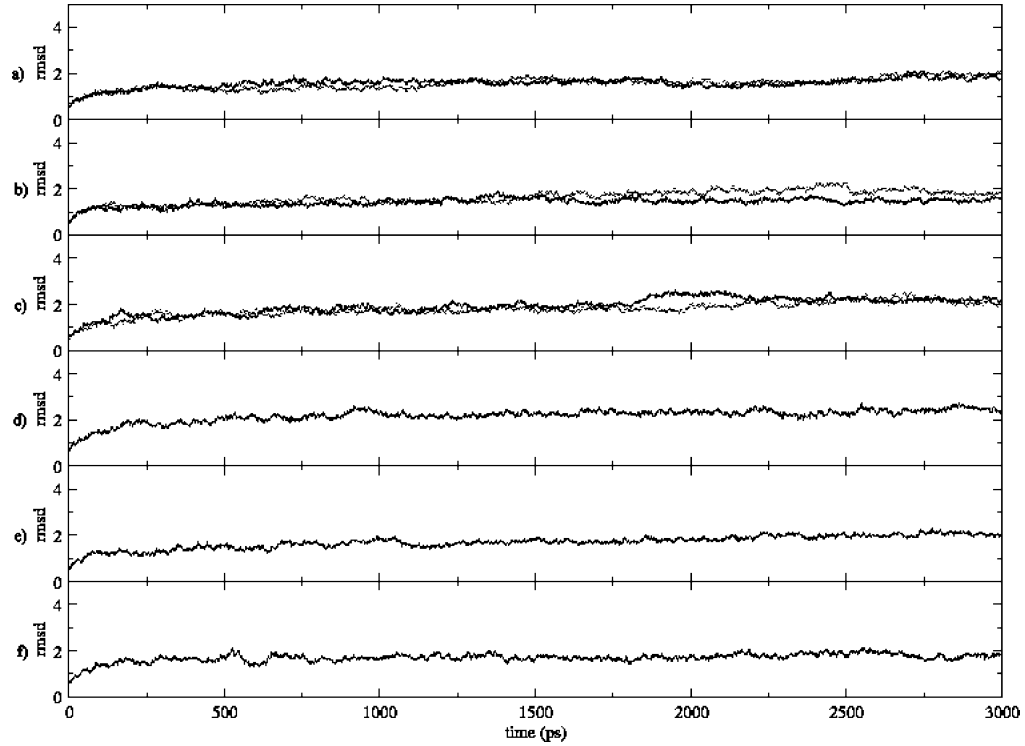

Figure 2. RMSD calculated along the MD trajectories for (a) **D**, (b) **DI**, (c) **D-I**, (d) **M**, (e) **MI**, and (f) **M-I**. In the a, b, and c plots, the black and gray lines correspond to monomers A and B, respectively.

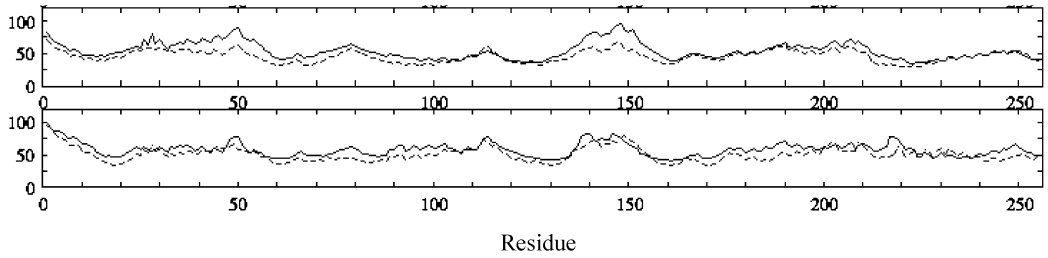

Figure 3. (Top) Calculated B factors for monomer A of **DI** (solid line) and monomer A of **D** (dashed line). (Bottom) Calculated B factors for **MI** (solid line) and **M** (dashed line).

L13. To obtain the complete set of coordinates, we added the missing residues to both monomers of **D-I**; this structure originated the starting points of MD trajectories of 3 ns for each model. Details for the model building and MD simulations can be found in ref 62. All calculations were performed using the AMBER7 package with the Cornell et al. force field.[53,54]

Results and Discussion

The Induced-Fit Mechanism. To assess the stability of the simulations, the root-mean-squared deviation (RMSD) of the Cα atoms for all models with respect to the corresponding starting structure was monitored (Figure 2). The results show that stable trajectories were obtained. Most importantly, the calculated isotropic temperature factor (*B*-factor) from the MD trajectories of **D** and **D-I** agree very well with the experimental data as previously reported.[50]

To analyze the changes in atomic fluctuations between the bound and unbound forms of the dimer and monomer of the protease, the calculated *B*-factors for **DI** and **D** and **MI** and **M** were plotted in Figure 3. In our models, the complex formation increases the mobility of atoms in different regions of the enzyme, but this is much more pronounced for the dimeric state. More specifically, residues 35−90 in αA, L3, β2, L4, β3, L5, and β4 and residues 130−160 in β5, L9, and β6, which are located around the active site, are more ordered in the free enzyme than in the noncovalent complex. The increase in fluctuations observed for these regions is associated with a loss of hydrogen bonds between protein residues. Figure 4 shows the residues 35−90 and 130−160 and the hydrogen bonds (dashed lines) with occupancy greater than 50% that are present in the **D** model but not in **DI**. This demonstrates that the inhibitor binding, before the formation of the covalent bond, has a significant impact on the protein dynamics.

Significant conformational changes were observed experimentally in the dimer upon covalent binding of peptidyl-activated carbonyl inhibitors.[48,49] As shown in our previous work,[50] the comparison between the average structures for the monomers A of **DI** and **D** indicates that the conformational changes are not associated with the adduct formation, but rather with the formation of the noncovalent complex.

Tong and co-workers[48] verified that, if the unbound and covalently bound dimeric states are superimposed using one

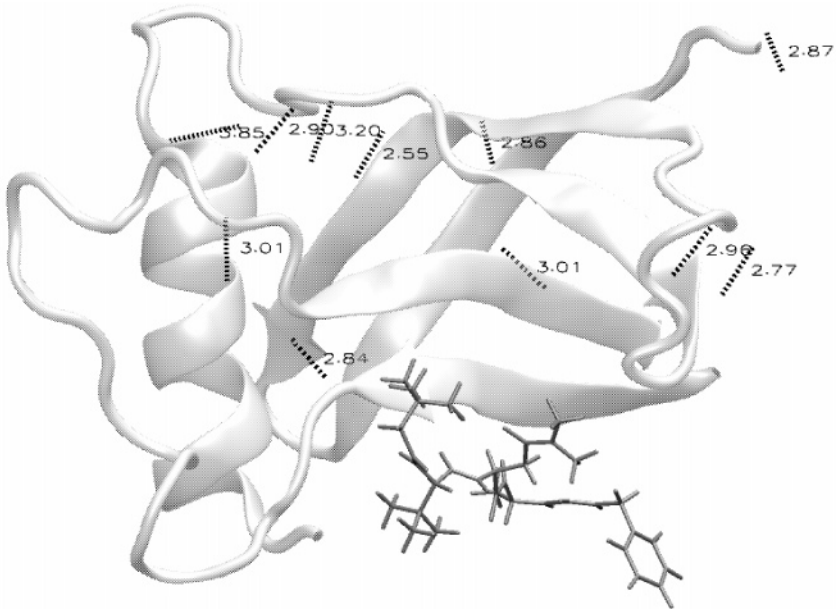

Figure 4. Cartoon representation of segments 35−90 and 130−160 for the **D** model. Dashed lines correspond to hydrogen bonds with occupancy greater than 50% found in the MD trajectory of **D**, but not in **DI**. To better localize the active site, the **D** and **DI** models were superimposed and only the inhibitor in **DI** is displayed.

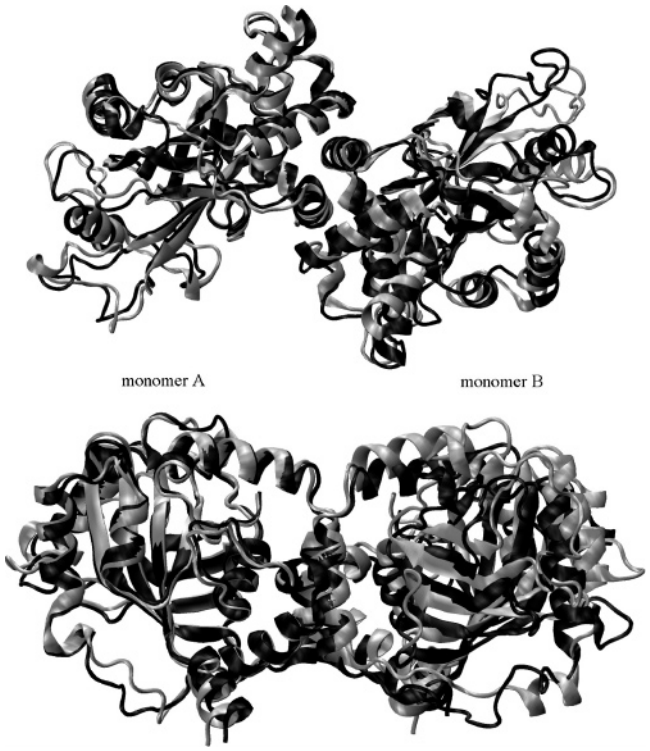

Figure 5. Superposition of the average structures obtained for **DI** (black) and **D** (gray) using monomer A as reference.

of the monomers as a reference, a rotation of 6.5° around an axis mostly perpendicular to the dimer 2-fold axis is needed to bring the second monomer into an overlapping position. This experimental observation was reproduced in our MD simulations of **D** and **DI**. It should be noted that the trajectories for **D** and **DI** were obtained using the crystal structure for the covalent complex as the starting point, which suggests that the sampling was adequate. Figure 5 shows the superposition of the average structures for **D** and **DI** using monomer A as a reference.

The cause of the change in the dimer organization is currently unknown. In order to investigate it, the following geometric parameters were monitored for the **DI** and **D** trajectories: (i) the distance between the center of mass of each monomer and (ii) the angle between the vectors V_1 and V_2, defined by the distance between the center of mass of each monomer in **DI** (V_1) and **D** (V_2) (Figure 6e)—in both models, the vector origins are the center of mass of monomer A; (iii) the angle defined by the centers of mass of monomer A, helices αF, and monomer B (AαFB; Figure 6f, left); and (iv) the dihedral angle defined by the center of mass of monomer A, the Cα atoms of Ser225 of helices αF of both monomers, and the center of mass of monomer B (Figure 6f, right).

Figure 6a shows that both **DI** and **D** have nearly the same distance between the centers of mass. Figure 6b shows that the angle between the vectors V_1 and V_2 oscillates around 6.0°. The noncovalent complex formation induces a rotation of monomer B around an axis mostly perpendicular to the dimer 2-fold axis, as shown in Figure 6c. After ca. 1 ns, the gap between the angles AαFB for **DI** and **D** oscillates around 5.0°, in excellent agreement with the experimental value of 6.5°. Finally, as can be seen in Figure 6d, the dihedral angle as defined above also changes upon noncovalent binding. Interestingly, the changes for this dihedral angle and the angle AαFB seem to be strongly correlated. As the angle AαFB for **D** becomes more linear, its dihedral angle becomes more planar. As the angle AαFB and the dihedral angle get closer to 180°, an increase in the distance between the centers of mass of monomers A and B should occur; this was not observed in the MD simulations. Therefore, a translation of monomer B with respect to monomer A must accompany

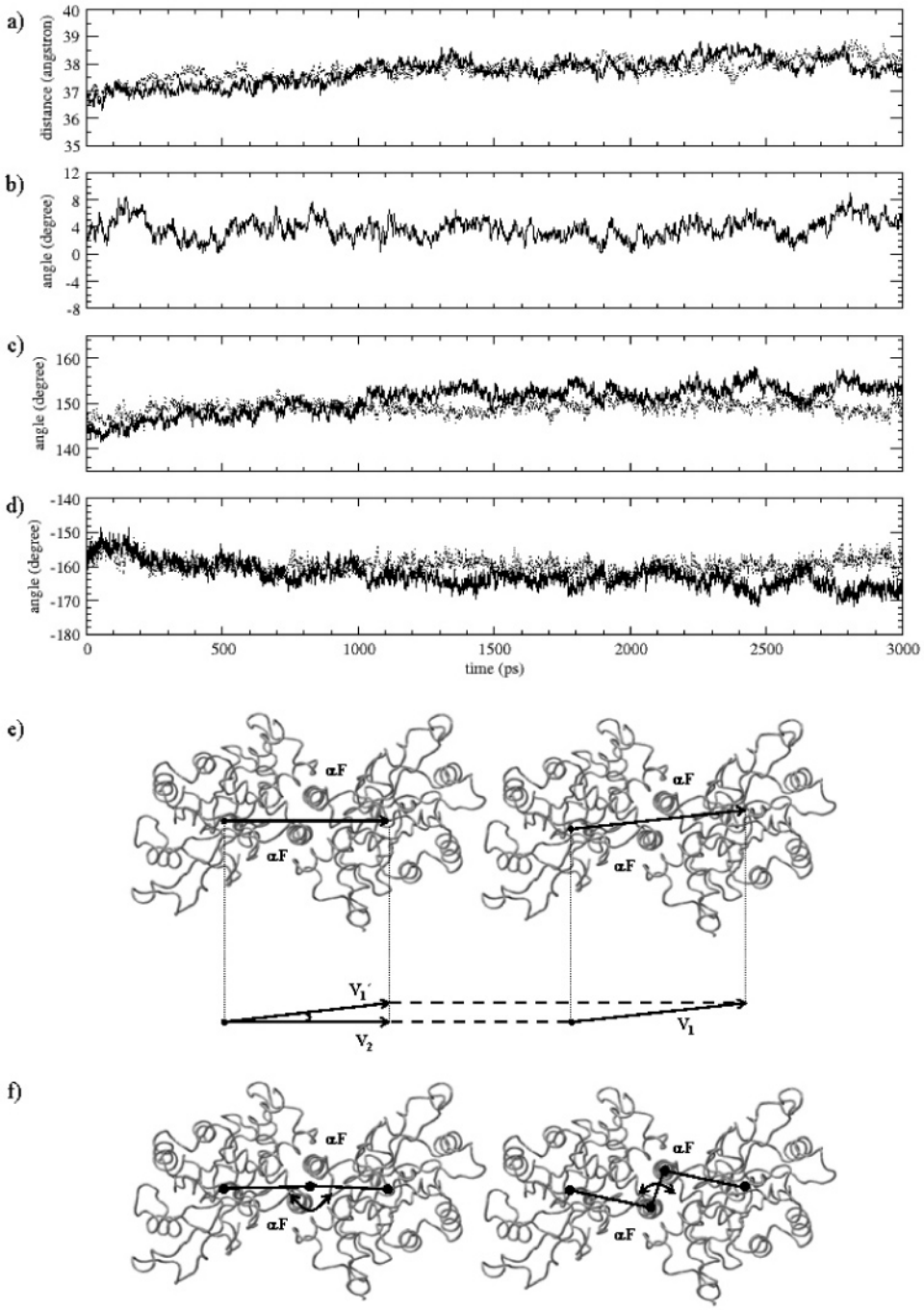

Figure 6. Plots corresponding to the time dependence of the following geometric parameters: (a) distance between the center of mass of each monomer; (b) angle between vectors V_1 and V_2, defined by the distance between the center of mass of each monomer in **DI** (V_1) and **D** (V_2); (c) angle defined by the centers of mass of monomer A, helices αF, and monomer B; (d) dihedral angle defined by the center of mass of monomer A, the Cα atoms of Ser225 of helices αF of both monomers, and the center of mass of monomer B; (e) schematic representation of vectors V_1, V_1', and V_2; (f) left, schematic representation of angle defined in c and, right, schematic representation of the dihedral angle defined in d. In graphics a, c, and d, solid and dashed lines correspond to the **D** and **DI** models, respectively.

the angle AαFB and the dihedral angle motions in order to keep the distance between the centers of mass roughly constant.

The changes in protein organization and conformation observed experimentally for the dimer covalently bound to BILC 821 were well-reproduced by the MD simulations of the noncovalent complex model, before the formation of the tetrahedral intermediate. This suggests that the HCMV protease operates by an induced-fit mechanism.[47]

Why is the Dimer Required for Catalytic Activity? Dynamic cross correlation matrix ($\mathbf{C}_{ij}$) was applied to study the collective motions related to the monomer−monomer interactions.[55−60] $\mathbf{C}_{ij}$ elements were obtained from their respective covariance matrix elements c_{ij} given by eq 1,

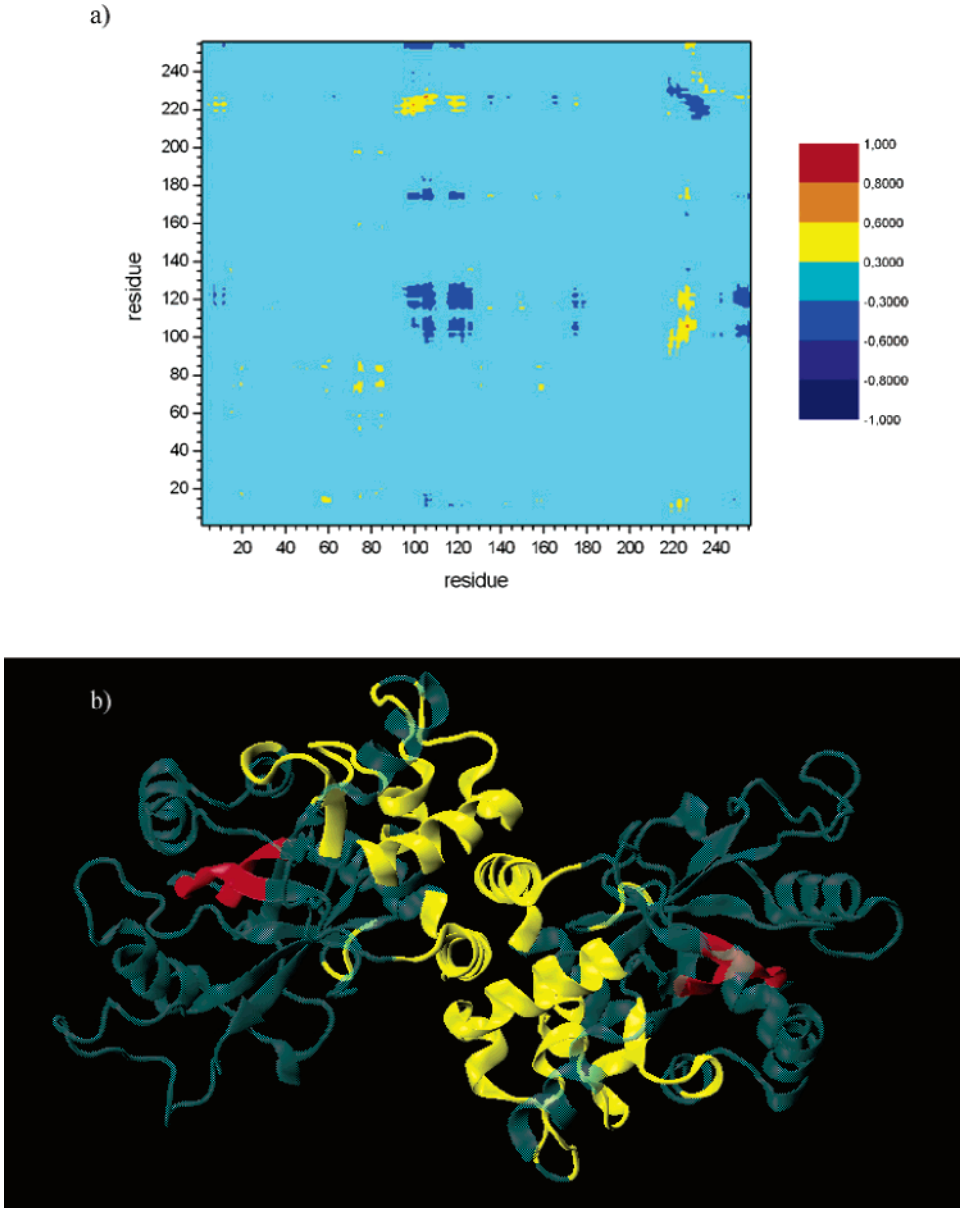

Figure 7. (a) Bidimensional representation of the dynamic cross correlation matrix elements calculated for **D**. Horizontal and vertical axes correspond to residues from monomers A and B, respectively. (b) Protease regions with intermonomer correlated motions are shown in yellow (interface) and red (active site).

where r_i is the atom i Cartesian coordinate vector and $< >$ represents a time average.

$$c_{ij} = \langle (r_i - \langle r_i \rangle)(r_j - \langle r_j \rangle) \rangle = \langle r_i \cdot r_j \rangle - \langle r_i \rangle \langle r_j \rangle \qquad (1)$$

When the c_{ij} terms are expanded, where t_{aver} is the time used to calculate the average value and Δt is the time interval between two consecutive configurations, eq 2 is obtained.

$$c_{ij} = \frac{\Delta t}{t_{aver}} \left\{ \sum_{t=0}^{t_{aver}-\Delta t} r_i(t)\, r_j(t) - \frac{\Delta t}{t_{aver}} \left[\sum_{t=0}^{t_{aver}-\Delta t} r_i(t)\, r_j(t) \right] \times \left[\sum_{t=0}^{t_{aver}-\Delta t} r_j(t)\, r_j(t) \right] \right\} \qquad (2)$$

Finally, the elements of the dynamic cross-correlation matrix, or normalized covariance, are defined as in eq 3.

$$\mathbf{C}_{ij} = \frac{c_{ij}}{c_{ii}^{1/2} c_{jj}^{1/2}} = \frac{\langle r_i \cdot r_j \rangle - \langle r_i \rangle \langle r_j \rangle}{[(\langle r_i^2 \rangle - \langle r_i \rangle^2)(\langle r_j^2 \rangle - \langle r_j \rangle^2)]^{1/2}} \qquad (3)$$

$\mathbf{C}_{ij}$ values vary from -1 to $+1$. Positive and negative values represent motions that are correlated and anticorrelated, respectively. The closer the value is to $+1$ or -1 for a pair of residues, the more correlated or anticorrelated their motions are, respectively. The dynamic cross-correlation matrix was calculated by averaging six blocks of 200 ps, with an offset of 50 ps, along the last 1.5 ns of the MD trajectories. To prevent the inclusion of spurious and artificially correlated motions,[55] the following residues were used in the fitting procedure: 13−23, 57−61, 67−78, 81−89, 130−134, 156−161, and 169−174 in the $\beta 1$−$\beta 7$ sheets

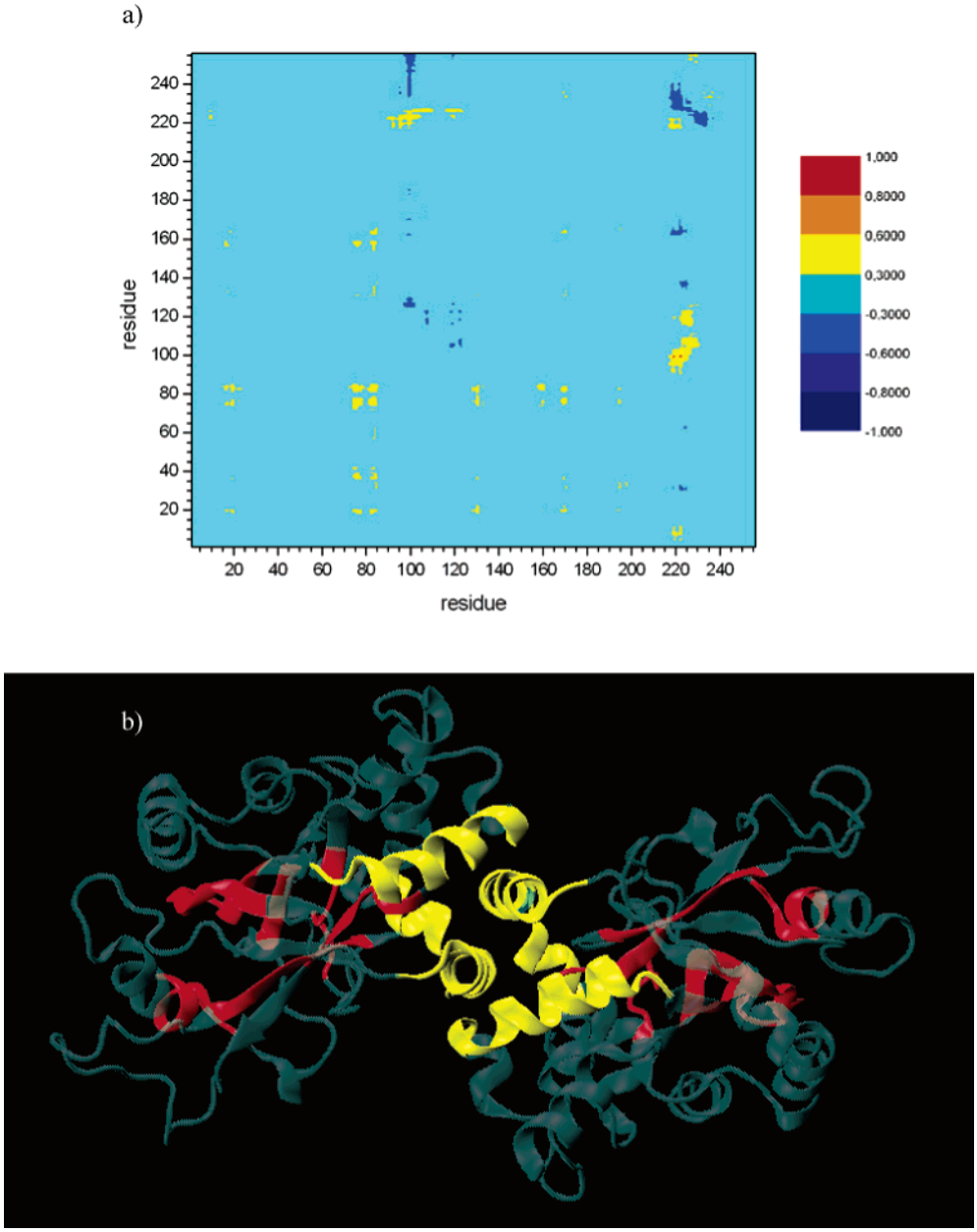

Figure 8. (a) Bidimensional representation of the dynamic cross correlation matrix elements calculated for **DI**. Horizontal and vertical axes correspond to residues from monomers A and B, respectively. (b) Protease regions with intermonomer correlated motions are shown in yellow (interface) and red (active site).

of both monomers. These residues are in the least flexible region of the protease.

Figures 7 and 8 show the dynamic cross-correlation matrix and the most relevant regions with intermonomer correlated motions obtained for the **D** and **DI** models, respectively. As expected, the intermonomer motions for residues close to the interface are strongly correlated (residues in yellow). Moreover, it was possible to identify correlated motions between residues from both active sites, which are separated by more than 30 Å (residues in red). Interestingly, while the correlated motions between residues located near the dimer interface decrease in **DI**, the noncovalent binding increases the number of intermonomer correlated motions between the active sites (Figures 7 and 8). Previous works claim that correlated and anticorrelated motions in the active site region may reduce the activation barrier through an increase in the number of reactive conformations sampled by the noncovalently bound complex.[56,61]

In order to investigate that, we monitored the interactions for the subsystem composed by the inhibitor and the catalytic triad in the noncovalently bound complex models. In both **DI** and **MI**, Ser132 is hydrogen-bonded to His63; the calculated distance between the Ser132 side-chain oxygen and His63 nitrogen $N\epsilon_2$ oscillates around 2.8 Å, while the angle $Ser_{132}O-Ser_{132}H-His_{63}N\epsilon_2$ fluctuates moderately around 170° (Chart 2). For both models, the His63 nitrogen $N\delta_1$ is hydrogen-bonded to His157 with occupancies of 62% for **DI** and 66% for **MI**. To verify whether Ser132 maintains its reactive orientation along the trajectories of **DI** and **MI**, we monitored the distance and the attacking angle between the Ser132 side-chain oxygen and the inhibitor's activated carbonyl group. In both models, the calculated distance

Chart 2. Representation of the Interactions Monitored for the Subsystem Composed by the Inhibitor and the Catalytic Triad in **MI** and **DI**

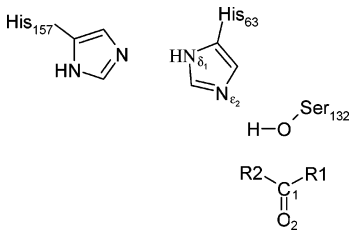

($Ser_{132}O-C_1$) and the angle ($Ser_{132}O-C_1-O_2$) fluctuate slightly around 2.9 Å and 95°, respectively (Chart 2). This seems to indicate that the presence of monomer−monomer interactions and correlated motions are not crucial to increase the number of reactive conformations and for the catalytic triad to orient properly in order to attack the inhibitor. Although the correlated motions between the active sites might not influence the activation barrier as discussed above, they still could have an impact in the reaction rate for the dimer by increasing its transmission factor. In other words, the presence of a network of coupled motions throughout the dimer would increase the probability of sampling conformations conducive to the catalyzed chemical reaction.[62]

In the crystal structure for the covalent complex between the protease and BILC 821, Arg165 interacts with the resulting oxyanion through its backbone NH. In addition, it has been suggested that the oxyanion is further stabilized by a water-mediated hydrogen bond with the side chain of Arg166.[63] Arg165 and Arg166 are highly conserved among all herpesvirus proteases. Liang and co-workers have shown through site-directed mutagenesis that, while the substitution of Arg166 by alanine has led to ablation of the enzymatic activity without detectable change in the HCMV protease conformation, the substitution of Arg165 by alanine revealed only a 2.7-fold reduction in activity.[63]

The role of these residues in the catalytic activity of the dimer was investigated by monitoring their interactions with the activated carbonyl oxygen of the inhibitor along the trajectories for **DI**, **D-I**, **MI**, and **M-I**. For Arg165, while the average distance between its backbone nitrogen and the carbonyl oxygen is ca. 2.9 Å for all models, the angle for this hydrogen bond changes significantly for **D-I**. Figure 9 shows that the angle distributions for the noncovalently and covalently bound complexes for the monomer are essentially the same. In the dimeric state, however, the angle distribution becomes narrower and its peak is shifted to more linear values upon formation of the oxyanion. A per-residue interaction energy analysis revealed that the more favorable interactions between the oxyanion and Arg165 translate into a reaction that is 7.0 kcal/mol more exergonic for the dimer, indicating a more significant thermodynamic driving force. The incipient oxyanion in the transition state should also benefit from the stronger interactions with Arg165, reducing the intrinsic barrier in the dimeric state. Quantum mechanics/molecular mechanics (QM/MM) simulations performed by our group show that the reaction is 6.6 kcal/mol more exothermic and the barrier is reduced by 8.1 kcal/mol in the dimeric state. The results also show that Arg165 is primarily responsible for it. This study will be published elsewhere.

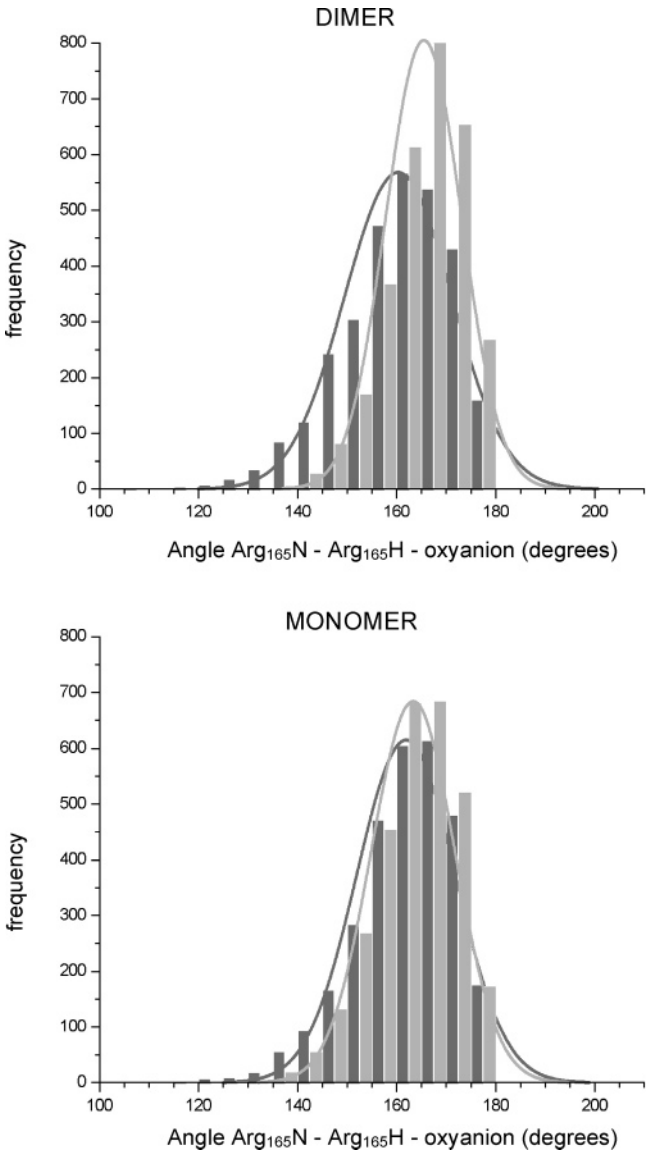

Figure 9. Arg_{165}**N**−Arg_{165}**H**−oxyanion angle distribution for the noncovalent (gray) and covalent complexes (light gray).

For Arg166, the water-mediated hydrogen bond between its side chain and the oxyanion has not been characterized in our MD simulations. In fact, no hydrogen bonds between Arg166 and the oxyanion were formed in any models (Figure 10). Also, the per-residue interaction energy analysis did not show any significant contribution from this residue to the catalytic activity of the dimer. Although our results are at odds with the results from mutagenesis experiments, the latter should be interpreted carefully. For example, the Arg166Ala mutation might abolish the enzymatic activity of the dimer not because important interactions between Arg166 and the oxyanion were lost but because of perturbations introduced by this mutation in the interactions with Arg165. In conclusion, our results suggest that only the dimeric form of the protease is able to reorient the main-chain atoms of Arg165 along the reaction coordinate in order to stabilize more efficiently the oxyanion formed in the reaction pathway.

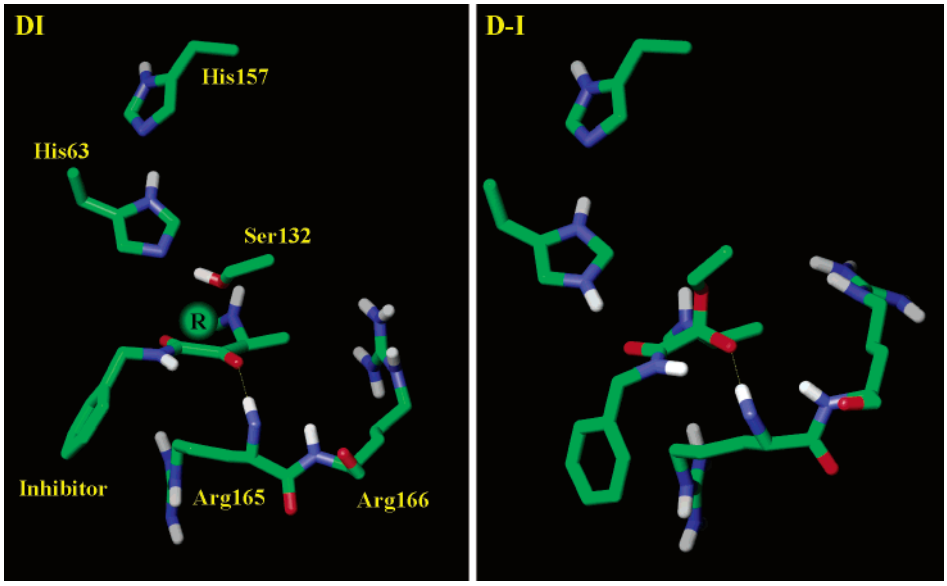

Figure 10. Noncovalently and covalently bound complexes for the dimeric state. The catalytic triad and the interactions between the inhibitor and Arg165 are illustrated. Parts of the inhibitor and other residues were excluded for clarity.

Conclusions

In this work, we used MD simulations to investigate the experimentally observed catalytic activity of the HCMV protease homodimer and the induced-fit mechanism upon the binding of substrates and peptidyl inhibitors. Long and stable trajectories were obtained for models of the monomeric and dimeric states, free in solution and bound covalently and noncovalently to a peptidyl-activated carbonyl inhibitor. Conformational changes observed experimentally for the dimer upon covalent binding were reproduced by the MD simulations of the noncovalent complex model, demonstrating that the HCMV protease operates by an induced-fit mechanism.

Dynamic cross-correlation analysis revealed that the noncovalent binding increases intermonomer correlated motions between residues of both active sites. The presence of a network of coupled motions throughout the enzyme could have a positive impact in the reaction rate for the dimer through the increase of its transmission factor. Finally, our results indicate that the catalytic activity of the dimer is a result of more favorable interactions between the oxyanion in the covalently bound state and the backbone nitrogen of Arg165, resulting in a reaction that is 7.0 kcal/mol more exergonic and a more significant thermodynamic driving force. The intrinsic activation barrier for the reaction in the dimeric state should also be reduced as the incipient oxyanion in the transition state would likely benefit from the stronger interactions with Arg165. This is supported by QM/MM simulations performed by our group, which shows that the activation barrier is reduced by 8.1 kcal/mol in the dimeric state. The results for this study will be published elsewhere.

Acknowledgment. This research has received partial financial support from the Brazilian agencies CNPq and FAPERJ (Grants 570535/1997-2 and E26-152174). C.A.F.O. acknowledges CNPq/Brazil and FAPERJ/Brazil for Ph. D. fellowships.

References

(1) Corey, L.; Spear, P. G. N. Infections with Herpes-Simplex Viruses 1. *N. Engl. J. Med.* **1986**, *314*, 686−691.

(2) Roizman, B.; Desrosiers, R. C.; Fleckenstein, B.; Lopez, C.; Minson, A. C.; Studdert, M. J. The Family Herpesviridae: An Update. *Arch. Virol.* **1992**, *123*, 425−449.

(3) Holwerda, B. C. Herpesvirus Proteases: Targets for Novel Antiviral Drugs. *Antiviral Res.* **1997**, *35*, 1−21.

(4) de Jong, M. D.; Galasso, G. J.; Gazzard, B.; Griffiths, P. D.; Jabs, D. A.; Kern, E. R.; Spector, S. A. Summary of the II International Symposium on Cytomegalovirus. *Antiviral Res.* **1998**, *39*, 141−162.

(5) Nichols, W. G; Boeckh, M. Recent Advances in the Therapy and Prevention of CMV Infections. *J. Clin. Virol.* **2000**, *16*, 25−40.

(6) Bruggeman, C. A.; Marjorie, H. J.; Nelissen-Vrancken, G. Cytomegalovirus and Atherogenesis. *Antiviral Res.* **1999**, *43*, 133−144.

(7) Jong, M. D.; Boucher, C. A. B.; Danner, S. A.; Gazzard, B.; Griffiths, P. D.; Katlama, C.; Lange, J. M. A.; Richman, D. D.; Vella, S. Summary of the International Consensus Symposium on Management of HIV, CMV and Hepatitis Virus Infections. *Antiviral Res.* **1998**, *37*, 1−16.

(8) Gilbert, C.; Boivin, G. Human Cytomegalovirus Resistance to Antiviral Drugs. *Antimicrob. Agents Chemother.* **2005**, *49*, 873−883.

(9) De Clercq, E. Antiviral Drugs in Current Clinical Use. *J. Clin. Virol.* **2004**, *30*, 115−133.

(10) De Clercq, E. New Inhibitors of Human Cytomegalovirus (HCMV) on the Horizon. *J. Antimicrob. Chemother.* **2003**, *51*, 1079−1083.

(11) De Clercq, E. Strategies in the Design of Antiviral Drugs. *Nat. Rev. Drug Discovery* **2002**, *1*, 13−25.

(12) De Clercq, E. Antiviral Drugs: Current State of the Art. *J. Clin. Virol.* **2001**, *22*, 73−89.

(13) Eizuru, Y. Development of New Antivirals for Herpesviruses. *Antiviral Chem. Chemother.* **2003**, *14*, 299−308.

(14) Emery, V. C. Progress in Understanding Cytomegalovirus Drug Resistance. *J. Clin. Virol.* **2001**, *21*, 223−228.

(15) Gibson, W.; Welch, A. R.; Hall, M. R. T. Assembling, a Herpes Virus Serine Maturational Proteinase and New Molecular Target for Antivirals. *Perspect. Drug Discovery Des.* **1994**, *2*, 413−426.

(16) Matusick-Kumar, L.; McCann, P. J.; Robertson, B. J.; Newcomb, W. W.; Brown, J. C.; Gao, M. Release of the Catalytic Domain N(o) from the Herpes Simplex Virus Type 1 Protease Is Required for Viral Growth. *J. Virol.* **1995**, *69*, 7113−7121.

(17) Gao, M.; Matusick-Kumar, L.; Hurlburt, W.; DiTusa, S. F.; Newcomb, W. W.; Brown, J. C.; McCann, P. J.; Deckman, I.; Colonno, R. J. The Protease of Herpes-Simplex Virus Type-1 Is Essential for Functional Capsid Formation and Viral Growth. *J. Virol.* **1994**, *68*, 3702−3712.

(18) Gopalsamy, A.; Lim, K.; Ellingboe, J. W.; Mitsner, B.; Nikitenko, A.; Upeslacis, J.; Mansour, T. S.; Olson, M. W.; Bebernitz, G. A.; Grinberg, D.; Feld, B.; Moy, F. J.; O'Connell, J. Design and Syntheses of 1,6-Naphthalene Derivatives as Selective HCMV Protease Inhibitors. *J. Med. Chem.* **2004**, *47*, 1893−1899.

(19) Borthwick, A. D.; Angier, S. J.; Crame, A. J.; Exall, A. M.; Haley, T. M.; Hart, G. J.; Mason, A. M.; Pennel, A. M. K; Weingarten, G. G. Design and Synthesis of Pyrrolidine-5,5-trans-lactams (5-Oxo-hexahydro-pyrrolo[3,2-b]pyrroles) as Novel Mechanism-Based Inhibitors of Human Cytomegalovirus Protease. 1. The Alpha-methyl-trans-lactam Template. *J. Med. Chem.* **2000**, *43*, 4452−4464.

(20) Dhanak, D.; Burton, G.; Christmann, L. T.; Darcy, M. G.; Elrod, K. C.; Kaura, A.; Keenan, R. M.; Link, J. O.; Peishoff, C. E.; Shah, D. H. Metal Mediated Protease Inhibition: Design and Synthesis of Inhibitors of the Human Cytomegalovirus (hCMV) Protease. *Bioorg. Med. Chem. Lett.* **2000**, *10*, 2279−2282.

(21) Dhanak, D.; Keenan, R. M.; Burton, G.; Kaura, A.; Darcy, M. G.; Shah, D. H.; Ridgers, L. H.; Breen, A; Lavery, P.; Tew, D. G.; West, A. Benzothiopyran-4-one Based Reversible Inhibitors of the Human Cytomegalovirus (HCMV) Protease. *Bioorg. Med. Chem. Lett.* **1998**, *8*, 3677−3682.

(22) Déziel, R.; Malefant, E. Inhibition of Human Cytomegalovirus Protease N-o with Monocyclic Beta-Lactams. *Bioorg. Med. Chem. Lett.* **1998**, *8*, 1437−1442.

(23) Yoakim, C.; Ogilvie, W. W.; Cameron, D. R.; Chabot, C.; Guse, I.; Haché, B.; Naud, J.; O'Meara, J. A.; Plante, R.; Déziel, R. Beta-Lactam Derivatives as Inhibitors of Human Cytomegalovirus Protease. *J. Med. Chem.* **1998**, *41*, 2882−2891.

(24) Pinto, I. L.; West, A.; Debouck, C. M.; DiLella, A. G.; Gorniak, J. G.; O'Donnel, K. C.; O'Shannessy, D. J.; Patel, A.; Jarvest, R. L. Novel, Selective Mechanism-Based Inhibitors of the Herpes Proteases. *Bioorg. Med. Chem. Lett.* **1996**, *6*, 2467−2472.

(25) Patick, A. K.; Potts, K. E. Protease Inhibitors as Antiviral Agents. *Clin. Microbiol. Rev.* **1998**, *11*, 614−627.

(26) Flynn, D. L.; Abood, N. A.; Holwerda, B. C. Recent Advances in Antiviral Research: Identification of Inhibitors of the Herpesvirus Proteases. *Curr. Opin. Chem. Biol.* **1997**, *1*, 190−196.

(27) Baum, E. Z.; Bebernitz, G. A.; Hulmes, J. D.; Muzithras, V. P.; Jones, T. R.; Gluzman, Y. Expression and Analysis of the Human Cytomegalovirus-UL80-Encoded Protease Identification of Autoproteolytic Sites. *J. Virol.* **1993**, *67*, 497−506.

(28) Gibson, W. Action at the Assemblin Dimer Interface. *Nat. Struct. Biol.* **2001**, *8*, 739−741.

(29) LaFemina, R. L.; Bakshi, K.; Long, W. J.; Pramanik, B.; Veloski, C. A.; Wolanski, B. S.; Marcy, A. I.; Hazuda, D. J. Characterization of a Soluble Stable Human Cytomegalovirus Protease and Inhibition by M-Site Peptide Mimics. *J. Virol.* **1996**, *70*, 4819−4824.

(30) Holwerda, B. C.; Wittwer, A. J.; Duffin, K. L.; Smith, C.; Toth, M. V.; Carr, L. S.; Wiegand, R. C.; Bryant, M. L. Activity of 2-Chain Recombinant Human Cytomegalovirus Protease. *J. Biol. Chem.* **1994**, *269*, 25911−25915.

(31) O'Boyle, D. R.; Wager-Smith, K.; Stevens, J. T.; Weinheimer, S. P. The Effect of Internal Autocleavage on Kinetic-Properties of the Human Cytomegalovirus Protease Catalytic Domain. *J. Biol. Chem.* **1995**, *270*, 4753−4758.

(32) Tong, L. Viral Proteases. *Chem. Rev.* **2002**, *102*, 4609−4626.

(33) Welch, A. R.; McNally, L. M.; Hall, M. R. T.; Gibson, W. Herpesvirus Proteinase - Site-Directed Mutagenesis Used to Study Maturational, Release, and Inactivation Cleavage Sites of Precursor and to Identify a Possible Catalytic Site Serine and Histidine. *J. Virol.* **1993**, *67*, 7360−7372.

(34) Reiling, K. K.; Pray, T. R.; Craik, C. S.; Stroud, R. M. Functional Consequences of the Kaposi's Sarcoma-Associated Herpesvirus Protease Structure: Regulation of Activity and Dimerization by Conserved Structural Elements. *Biochemistry* **2000**, *39*, 12796−12803.

(35) Hoog, S. S.; Smith, W. W.; Qiu, X. Y.; Janson, C. A.; Hellmig, B.; McQueney, M. S.; ODonnell, K.; OShannessy, D.; DiLella, A. G.; Debouck, C.; AbdelMeguid, S. S. Active Site Cavity of Herpesvirus Proteases Revealed by the Crystal Structure of Herpes Simplex Virus Protease/Inhibitor Complex. *Biochemistry* **1997**, *36*, 14023−14029.

(36) Qiu, X.; Janson, C. A.; Culp, J. S.; Richardson, S. B.; Debouck, C.; Smith, W. W.; Abdel-Meguid, S. S. Crystal Structure of Varicella-Zoster Virus Protease. *Proc. Natl. Acad. Sci. U. S. A.* **1997**, *94*, 2874−2879.

(37) Chen, P.; Tsuge, H.; Almassy, R. J.; Gribskov, C. L.; Katoh, S.; Vanderpool, D. L.; Margosiak, S. A.; Pinko, C.; Matthews, D. A.; Kan, C. Structure of the Human Cytomegalovirus Protease Catalytic Domain Reveals a Novel Serine Protease Fold and Catalytic Triad. *Cell* **1996**, *86*, 835−843.

(38) Qiu, X.; Culp, J. S.; DiLella, A. G.; Hellmig, B.; Hoog, S. S.; Janson, C. A.; Smith, W. W.; Abdel-Meguid, S. S. Unique Fold and Active Site in Cytomegalovirus Protease. *Nature* **1996**, *383*, 275−279.

(39) Shieh, H. S.; Kurumbail, R. G.; Stevens, A. M.; Stegeman, R. A.; Sturman, E. J.; Pak, J. Y.; Wittwer, A. J.; Palmier, M. O.; Wiegand, R. C.; Holwerda, B. C.; Stallings, W. C. Three Dimensional Structure of Human Cytomegalovirus Protease. *Nature* **1996**, *383*, 279−282.

(40) Tong, L.; Qian, C.; Massariol, M-J.; Bonneau, P.; Cordingley, M.; Lagacé, L. A New Serine-Protease Fold Revealed by the Crystal Structure of Human Cytomegalovirus Protease. *Nature* **1996**, *383*, 272−275.

(41) Khayat, R.; Batra, R.; Massariol, M.-J.; Lagacé, L.; Tong, L. Investigating the Role of Histidine 157 in the Catalytic Activity of Human Cytomegalovirus Protease. *Biochemistry* **2001**, *40*, 6344−6351.

(42) Hedstrom, L. Serine Protease Mechanism and Specificity. *Chem. Rev.* **2002**, *102*, 4501−4523.

(43) Dereweda, Z. S.; Dereweda, U.; Kobos, P. M. (His)C−Epsilon−H···O═C Hydrogen-Bond in the Active-Sites of Serine Hydrolases. *J. Mol. Biol.* **1994**, *241*, 83−93.

(44) Carter, P.; Wells, J. A. (His)C−Epsilon−H···O═C Hydrogen-Bond in the Active-Sites of Serine Hydrolases. *Nature* **1988**, *332*, 564−568.

(45) Neurath, H. Evolution of Proteolytic-Enzymes. *Science* **1984**, *224*, 350−357.

(46) Kraut, J. Serine Proteases - Structure and Mechanism of Catalysis. *Annu. Rev. Biochem.* **1977**, *46*, 331−358.

(47) LaPlante, S. R.; Bonneau, P. R.; Aubry, N.; Cameron, D. R.; Deziel, R.; Grand-Maitre, E.; Plouffe, C.; Tong, L.; Kawai, S. H. Characterization of the Human Cytomegalovirus Protease as an Induced-Fit Serine Protease and the Implications to the Design of Mechanism-Based Inhibitors. *J. Am. Chem. Soc.* **1999**, *121*, 2974−2986.

(48) Tong, L.; Qian, C.; Massariol, M.-J.; Déziel, R.; Yoakim, C.; Lagacé, L. Conserved Mode of Peptidomimetic Inhibition and Substrate Recognition of Human Cytomegalovirus Protease. *Nat. Struct. Biol.* **1998**, *5*, 819−826.

(49) Bonneau, P. R.; Grand-Maître, C.; Greenwood, D. J.; Lagacé, L.; LaPlante, S. R.; Massariol, M.-J.; Ogilvie, W. W.; O'Meara, J. A.; Kawai, S. H. Evidence of a Conformational Change in the Human Cytomegalovirus Protease upon Binding of Peptidyl-Activated Carbonyl Inhibitors. *Biochemistry* **1997**, *36*, 12644−12652.

(50) de Oliveira, C. A. F.; Guimarães, C. R. W.; Barreiro, G.; Alencastro, R. B. Investigation of the Induced-Fit Mechanism and Catalytic Activity of the Human Cytomegalovirus Protease Homodimer via Molecular Dynamics Simulations. *Proteins* **2003**, *52*, 483−491.

(51) Batra, R.; Khayat, R.; Tong, L. Molecular Mechanism for Dimerization to Regulate the Catalytic Activity of Human Cytomegalovirus Protease. *Nat. Struct. Biol.* **2001**, *8*, 810−817.

(52) Darke, P. L.; Cole, J. L.; Waxman, L.; Hall, D. L.; Sardana, M. K.; Kuo, L. C. Active Human Cytomegalovirus Protease is a Dimer. *J. Biol. Chem.* **1996**, *271*, 7445−7449.

(53) Case, D. A.; Perlman, D. A.; Caldwell, J. W.; Chetham, T. E., III; Ross, W. S.; Simmerling, C. L.; Darden, T. A.; Merz, K. M.; Stanton, R. V.; Cheng, A. L.; Vincent, J. J.; Crowley, M.; Tsui, V.; Gohlke, H.; Radmer, R. J.; Duan, Y.; Pitera, J.; Massova, I.; Seibel, G. L.; Singh, U. C.; Weiner, P. K.; Kollman, P. A. *AMBER 7*; University of California: San Francisco, CA, 1995.

(54) Cornell, W. D.; Cieplak, P.; Bayly, C. I.; Gould, I. R.; Merz, K. M., Jr.; Ferguson, D. M.; Spellmeyer, D. C.; Fox, T.; Caldwell, J. W.; Kollman, P. A. A 2nd Generation Force-Field for the Simulation of Proteins, Nucleic-Acids, and Organic-Molecules. *J. Am. Chem. Soc.* **1995**, *117*, 5179−5197.

(55) Hunenberger, P. H.; Mark, A. E.; Gunsteren, W. F. Fluctuation and Cross-Correlation Analysis of Protein Motions Observed in Nanosecond Molecular-Dynamics Simulations. *J. Mol. Biol.* **1995**, *252*, 492−503.

(56) Estabrook, R. A.; Luo, J.; Purdy, M. M.; Sharma, V.; Weakliem, P.; Bruice, T. C.; Reich, N. O. Statistical Coevolution Analysis and Molecular Dynamics: Identification of Amino Acid Pairs Essential for Catalysis. *Proc. Natl. Acad. Sci. U. S. A.* **2005**, *102*, 994−999.

(57) Mazumder-Shivakumar, D.; Bruice, T. C. Computational Study of IAG-Nucleoside Hydrolase: Determination of the Preferred Ground State Conformation and the Role of Active Site Residues. *Biochemistry* **2005**, *44*, 7805−7817.

(58) Zoete, V.; Meuwly, M.; Karplus, M. A Comparison of the Dynamic Behavior of Monomeric and Dimeric Insulin Shows Structural Rearrangements in the Active Monomer. *J. Mol. Biol.* **2004**, *342*, 913−929.

(59) Harte, W. E., Jr.; Swaminathan, S.; Beveridge, D. Molecular Dynamics of HIV-1 Protease. *Proteins* **1992**, *13*, 175−194.

(60) Ichiye, T.; Karplus, M. Collective Motions in Proteins: A Covariance Analysis of Atomic Fluctuations in Molecular Dynamics and Normal Mode Simulations. *Proteins* **1991**, *11*, 205−217.

(61) Luo, J.; Bruice, T. C. Ten-Nanosecond Molecular Dynamics Simulation of the Motions of the Horse Liver Alcohol Dehydrogenase. PhCH2O- complex. *Proc. Natl. Acad. Sci. U. S. A.* **2002**, *99*, 16597−16600.

(62) Hammes-Schiffer, S.; Benkovic, S. J. Relating Protein Motion to Catalysis. *Annu. Rev. Biochem.* **2006**, *75*, 519−541.

(63) Liang, Po-H.; Brun, K. A.; Feild, J. A.; O'Donnell, K.; Doyle, M. L.; Green, S. M.; Baker, A. E.; Blackburn, M. N.; Abdel-Meguid, S. S. Site-Directed Mutagenesis Probing the Catalytic Role of Arginines 165 and 166 of Human Cytomegalovirus Protease. *Biochemistry* **1998**, *37*, 5923−5929.

CT600175X